CHEMISTRY
A EUROPEAN JOURNAL

DOI: 10.1002/chem.200600069

Structural Development of Free or Coordinated 4′-(4-Pyridyl)-2,2′:6′,2″-terpyridine Ligands through N-Alkylation: New Strategies for Metallamacrocycle Formation

Edwin C. Constable,*[a] Emma L. Dunphy,[a] Catherine E. Housecroft,[a] William Kylberg,[a] Markus Neuburger,[a] Silvia Schaffner,[a] Emma R. Schofield,[a] and Christopher B. Smith[a, b]

Abstract: A series of N-alkylated derivatives of $[Ru(pytpy)_2]^{2+}$ (pytpy = 4′-(4-pyridyl)-2,2′:6′,2″-terpyridine) has been synthesised and characterised. These include both model and functionalised complexes that complement previously reported iron(II) analogues. Reaction of $[Ru(pytpy)_2]^{2+}$ with bis[4-(bromomethyl)phenyl]methane leads to the formation of a [2+2] ruthenamacrocycle. Related ferramacrocycles could not be accessed by this route, and instead were prepared in two steps by first reacting bis[4-(bromomethyl)-phenyl]methane or 4,4′-bis(bromomethyl)biphenyl with two equivalents of pytpy, and then treating the resulting bis(N-alkylated) product with iron(II) salts.

Keywords: alkylation · heterocycles · iron · metallacycles · ruthenium

Introduction

Multitopic ligands that contain two or more 2,2′:6′,2″-terpyridine (tpy) metal-binding domains are now well established as building-blocks for the assembly of supramolecular systems.[1,2] While bipyridine (bpy) metal-binding domains are also commonly used,[3] their disadvantage is that they give rise to chiral (Δ and Λ) [*cis*-$M(bpy)_2X_2$] and $[M(bpy)_3]$ species. In contrast, tpy ligands substituted at the 4′-position, or symmetrically on the outer rings, give achiral $[M(tpy)_2]$ complexes.[4] Metal-directed self-assembly based on the coordination chemistry of ditopic tpy ligands has received significant recent attention. In most cases, metallamacrocycles are formed by the reaction of the ditopic tpy ligand with metal ions, but a significant problem is the competition between the formation of metallamacrocycles (often entropically favoured under conditions of high dilution)[5–22] and metallapolymers.[22–28] Designing spacers between the metal-bonding domains that possess appropriate structural coding is one strategy for driving the reaction towards metallamacrocycle rather than polymer formation. This has been demonstrated by Newkome and co-workers in both the assembly of molecular triangles[13] and hexagons.[7,9,10,14] Conversely, the use of flexible spacers that impose little restriction in conformational space, appears to favour metallapolymer formation.[22–28] In our own work, we have demonstrated the formation of a range of metallamacrocycles with less well preorganised ligands,[15–19,21] but have also shown that the 78° angle between the least-squares planes of the two central pyridine rings in tpySStpy preorganises the ligand for the formation of a [4+4] metallamacrocycle upon reaction with iron(II) salts.[20] In this report, we focus attention on the use of 4′-(4-pyridyl)-2,2′:6′,2″-terpyridine (pytpy) as a building block in supramolecular chemistry.

The pytpy ligand[29] exhibits versatile coordination chemistry, forming mononuclear complexes with one or two pendant pyridine groups,[29–37] coordination polygons,[38,39] and coordination polymers.[40,41] The pendant pyridine donor has been used to control the self-assembly of monolayers on platinum, the monolayers being investigated by scanning tunnelling microscopy and electrochemical techniques.[31,42,43] Some years ago, we presented a preliminary report of a

[a] Prof. Dr. E. C. Constable, E. L. Dunphy, Prof. Dr. C. E. Housecroft, W. Kylberg, M. Neuburger, Dr. S. Schaffner, Dr. E. R. Schofield, Dr. C. B. Smith
Department of Chemistry, University of Basel
Spitalstrasse 51, 4056 Basel (Switzerland)
Fax: (+41) 61-267-1005
E-mail: edwin.constable@unibas.ch

[b] Dr. C. B. Smith
Current address:
School of Biomedical, Biomolecular and Chemical Sciences
University of Western Australia, Crawley
Perth, W.A. 6009 (Australia)

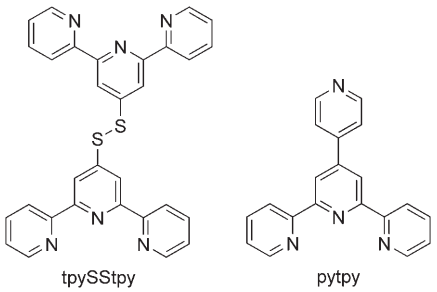

strategy for the construction of a [2+2] metallamacrocycle containing {Fe(tpy)$_2$} motifs based on the N-alkylation of the pendant pyridine ring in coordinated pytpy.[5] We have also described a series of N-alkylation reactions of the 4′-pyridyl groups in [M(pytpy)$_2$]$^{2+}$ that allow the introduction of functional substituents to generate a series of metallaviologens analogous to viologens.[29,30,44] The strategy of N-alkylation of free and coordinated pytpy has potential for use in a range of applications. Williams and co-workers have observed that iridium(III)–bis(tpy) complexes containing 4′-(3-*N*-methylpyridyl) or 4′-(4-*N*-methylpyridyl) substituents function as luminescent sensors for chloride ions,[45] and Loeb has shown that the N-alkylation of pytpy by 1-bromo-2-(4,4′-bipyridinium)ethane bromide leads to an effective building block for the axle of a [2]-rotaxane that has the capability of binding metal ions.[46] In an elegant piece of work, Kurth has reported the assembly of a pytpy-based cobalt(II)–metallaviologen[47] that has been incorporated as a functional component of electrochromic thin films.[48–50] This diversity of applications of N-alkylated pytpy ligands leads us to present a full account of our recent activities in this area.

Results and Discussion

Model N-alkyl derivatives of [Ru(pytpy)$_2$]$^{2+}$: We have previously reported the preparation, characterisation and reactivity of a series of complexes formed by the N-alkylation of [Fe(pytpy)$_2$]$^{2+}$ (**1**$^{2+}$).[29,44] These studies confirmed that **1**$^{2+}$ behaves in an analogous manner to 4,4′-bipyridine, undergoing N-alkylation reactions at both non-coordinated nitrogen atoms to produce metallaviologens.[5] A crystallographic study of the N-benzylated derivative [Fe(*N*-PhCH$_2$pytpy)$_2$]-[PF$_6$]$_4$[44] illustrated that the spatial properties of [Fe(*N*-PhCH$_2$pytpy)$_2$]$^{4+}$ render it and its related complexes ideal building blocks for the formation of metallamacrocyclic complexes from cyclic bis(4,4′-bipyridinium) salts.[51] We have now extended our investigation of model N-alkylated complexes to the reactions of [Ru(pytpy)$_2$]$^{2+}$ (**2**$^{2+}$),[30] with a range of alkylating agents.

We have previously shown that whereas **1**$^{2+}$ readily reacts with MeI to give [Fe(*N*-Mepytpy)$_2$]$^{4+}$ (*N*-Mepytpy = 4′-(*N*-methyl-4-pyridinio)-2,2′:6′,2″-terpyridine), N-methylation of **2**$^{2+}$ requires an excess of [Me$_3$O][BF$_4$] in CH$_3$CN under reflux.[30] The reaction of **2**[PF$_6$]$_2$ with an excess of benzyl bromide in CH$_3$CN at reflux proceeded smoothly to give, after workup, **3**[PF$_6$]$_4$ as a pink solid in 68% yield. The elec-

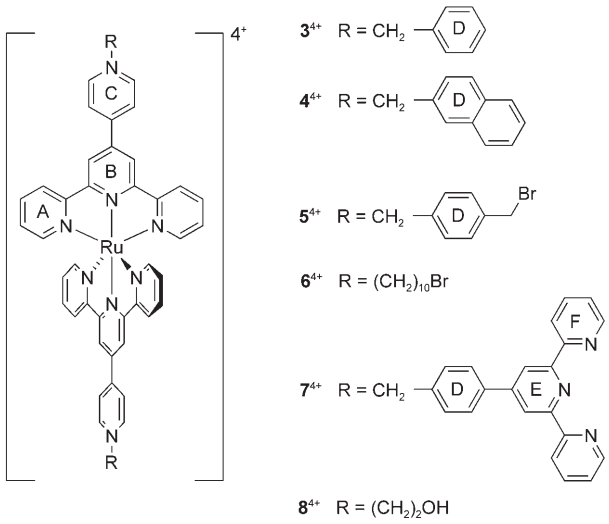

trospray (ES) mass spectrum exhibited peak envelopes at $m/z = 1339$ ([M−PF$_6$]$^+$) and 597 ([M−2PF$_6$]$^{2+}$) and a base peak in the mass spectrum at $m/z = 362$ ([Ru(pytpy)$_2$]$^{2+}$). Each envelope showed the correct distribution of isotopologues. The ^{1}H and ^{13}C NMR spectra of **3**[PF$_6$]$_4$ confirmed a symmetrical product and were fully assigned by using COSY, HMBC, and HMQC techniques. In terms of the signals assigned to the pytpy protons, the ^{1}H NMR spectrum is very similar to that of [Ru(*N*-Mepytpy)$_2$][PF$_6$]$_4$,[30] with only signals for H^{3B}, H^{2C} and H^{3C} showing significant differences between **2**$^{2+}$ and **3**$^{4+}$ (Table 1). Of these, the signal for proton H^{3C} undergoes the largest change, moving 0.53 ppm to higher frequency. Confirmation that N-alkylation had occurred at both pendant pyridine rings came from the results of a single-crystal structure determination of the complex. Crystals of **3**[PF$_6$]$_4$·2(CH$_3$)$_2$CO·$^1/_3$CH$_3$CN were grown by slow diffusion of diethyl ether into a solution of **3**[PF$_6$]$_4$ in acetonitrile/acetone . Although the crystal quality was poor, it was sufficient to permit the gross structural features of **3**[PF$_6$]$_4$ to be confirmed. The molecular structure of the **3**$^{4+}$ ion is presented in Figure 1 (top), and selected bond lengths and angles are given in the caption. The bond lengths and angles within the {Ru(tpy)$_2$} moiety are unexceptional. Of the four [PF$_6$]$^-$ ions, one has each F atom disordered over two sites, each with 50% occupancy. One of the acetone solvent molecules is disordered over two positions (1:1), with one site coinciding with the position of the 33% occupancy acetonitrile molecule. In the solid state, two types of interaction between **3**$^{4+}$ ions are important. Firstly, rows of cations run parallel to the crystallographic *a* axis, with the cations in each row off-set from one another to facilitate π-stacking between pyridine rings containing atoms N4 and N6 of adjacent cations (shortest contacts between planes = 3.5 Å). Complementing this arrangement is one in which cations align parallel to the *b* axis (Figure 1 bottom) so that there

Table 1. ^{1}H NMR spectroscopic data [δ in ppm] for CD_3CN solutions of pytpy and symmetrical ruthenium(II) and iron(II) complexes. See schematic diagrams and Schemes 2 and 3 for compound numbering and ring labelling.

	H^{3A}	H^{4A}	H^{5A}	H^{6A}	H^{3B}	H^{2C}	H^{3C}
pytpy[a]	8.72	7.99	7.47	8.74	8.80	8.77	7.83
ruthenium(II) complexes							
2$[PF_6]_2$[a]	8.66	7.97	7.20	7.43	9.07	8.97	8.14
$[Ru(N\text{-Mepytpy})_2][PF_6]_4$[a]	8.68	8.01	7.23	7.43	9.13	8.95	8.72
3$[PF_6]_4$	8.70	8.00	7.23	7.43	9.14	9.09	8.77
4$[PF_6]_4$	8.72	7.99	7.22	7.43	9.19	9.18	8.83
5$[PF_6]_4$	8.70	8.00	7.22	7.43	9.16	9.11	8.78
6$[PF_6]_4$	8.72	8.01	7.23	7.45	9.19	9.04	8.78
7$[PF_6]_4$	8.70 (8.72, H^{3F})	8.00 (8.04, H^{4F})	7.22 (7.52, H^{5F})	7.43 (8.74, H^{6F})	9.18 (8.79, H^{3E})	9.17	8.80
8$[PF_6]_4$	8.69	8.01	7.24	7.44	9.15	9.03	8.76
16$[PF_6]_8$	8.55	7.54	6.63	7.28	9.12	9.00	8.75
iron(II) complexes							
1$[BF_4]_2$[b]	8.63	7.92	7.09	7.17	9.23	9.03	8.23
$[Fe(N\text{-}PhCH_2pytpy)_2][PF_6]_4$[c]	8.63	7.96	7.13	7.18	9.27	9.13	8.82
14$[PF_6]_8$	8.50	7.80	6.99	7.01	9.16	9.14	8.76
15$[PF_6]_8$	8.44	7.44	6.52	6.99	9.19	9.03	8.78

[a] Reference [30]. [b Reference [29]. [c] Reference [44].

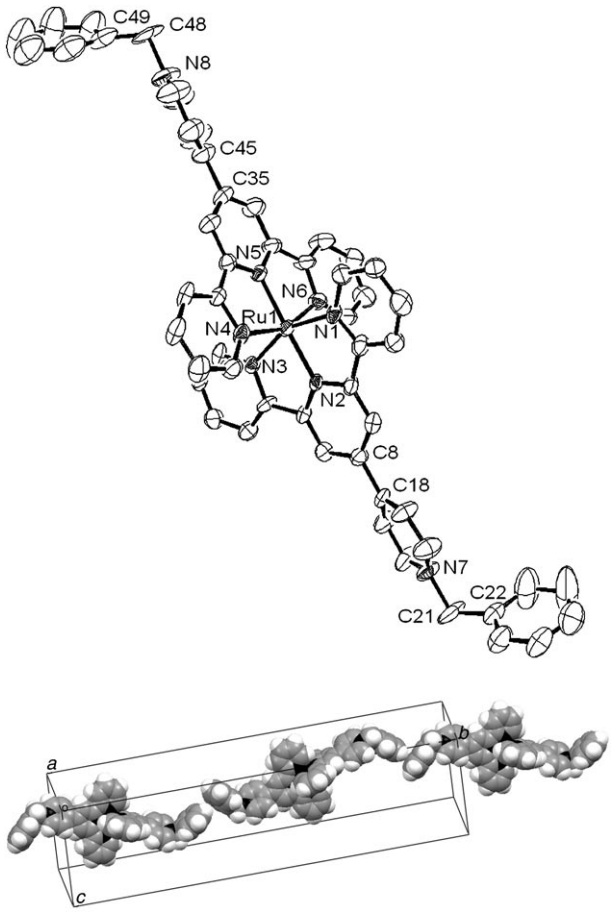

Figure 1. Top: Molecular structure of the $\mathbf{3}^{4+}$ ion in the complex $\mathbf{3}[PF_6]_4{\cdot}2(CH_3)_2CO{\cdot}0.3\,CH_3CN$. Selected bond parameters: Ru1–N1 = 2.064(5), Ru1–N2 = 1.966(5), Ru1–N3 = 2.066(5), Ru1–N4 = 2.073(5), Ru1–N5 = 1.970(5), Ru1–N6 = 2.080(5), C8–C18 = 1.484(8), N7–C21 = 1.500(9), C35–C45 = 1.493(10), N8–C48 = 1.486(9) Å; N1-Ru1-N2 = 79.0(2), N2-Ru1-N3 = 78.1(2), N4-Ru1-N5 = 78.6(2), N5-Ru1-N6 = 79.1(2), N7-C21-C22 = 114.8(7), N8-C48-C49 = 109.8(8)°. Bottom: Part of one chain of cations that pack along the *b* axis, supported by weak edge-to-face aromatic interactions.

are weak edge-to-face interactions[52,53] between benzyl aromatic rings (H521–centroid of ring containing atom C22 = 3.1 Å; angle C52-H521-centroid = 155.4°). These interactions control the relative orientations of the benzyl groups in the crystalline solid. Interestingly, similar edge-to-face interactions between benzyl groups are absent in the solid-state structure of the iron(II) analogue[44] and, as a result, the relative orientations of the benzyl groups differ between the iron(II) and ruthenium(II) complexes.

A second N-alkylated derivative of $\mathbf{2}^{2+}$ was prepared by the reaction of $\mathbf{2}[PF_6]_2$ with an excess of 2-bromomethylnaphthalene in CH_3CN under reflux. The reaction was monitored by TLC and had reached completion after 24 h. After chromatographic workup $\mathbf{4}[PF_6]_4$ was isolated in 71% yield. The electrospray mass spectrum of $\mathbf{4}[PF_6]_4$ showed peak envelopes at 1439 ($[M-PF_6]^+$), 1294 ($[M-2PF_6]^+$), 1152 ($[M-(napCH_2)-2PF_6]^+$), 867 ($[Ru(pytpy)_2(PF_6)]^+$) and 722 ($[Ru(pytpy)_2]^+$), each with the correct isotope distribution. The ^{1}H NMR spectrum of $\mathbf{4}[PF_6]_4$ is similar to that of $\mathbf{3}[PF_6]_4$, and both the ^{1}H and ^{13}C NMR spectra confirmed the presence of a symmetrical, homotopic complex. In addition to the ^{1}H NMR signals listed in Table 1, a singlet at δ = 6.07 ppm was assigned to the CH_2 group, and signals at δ = 8.17, 8.07, 8.01 and 7.66 ppm to the naphthalene protons.

The electronic absorption spectra of solutions of the two complexes $\mathbf{3}[PF_6]_4$ and $\mathbf{4}[PF_6]_4$ in CH_3CN resemble that of $[Ru(N\text{-Mepytpy})_2][PF_6]_4$.[30] Alkylation of $\mathbf{2}[PF_6]_2$ results in a red shift of the MLCT absorption from 488 nm in $\mathbf{2}[PF_6]_2$ to 507 nm in $[Ru(N\text{-Mepytpy})_2][PF_6]_4$,[30] 511 nm in $\mathbf{3}[PF_6]_4$ and 513 nm in $\mathbf{4}[PF_6]_4$. Each complex also shows a series of intense bands in the UV region that are assigned to ligand-centred $\pi^*\leftarrow\pi$ transitions; the absorption at 224 nm for $\mathbf{4}[PF_6]_4$ arises from the naphthalene group.

Both $\mathbf{3}[PF_6]_4$ and $\mathbf{4}[PF_6]_4$ are redox active and were studied by using cyclic and differential pulse voltammetries. We have previously reported that on going from $[Ru(tpy)_2][PF_6]_2$ to $[Ru(pytpy)_2][PF_6]_2$, there is a small shift to positive potential (+0.92 to +0.95 V) for the Ru^{2+}/Ru^{3+} oxidation

process, indicating that the 4-pyridyl substituent is very weakly electron-withdrawing.[30] Methylation of the pendant pyridyl groups results in a further shift to +1.03 V, consistent with an increase in the electron-withdrawing effect on going from pytpy to [*N*-Mepytpy]$^+$.[30] For **3**[PF_6]$_4$ and **4**[PF_6]$_4$, metal-centred oxidation processes were observed at +1.01 and +1.02 V, respectively, illustrating that the benzyl and naphthylmethyl substituents behave in a similar manner to the methyl substituent in [Ru(*N*-Mepytpy)$_2$]$^{4+}$. Each of **3**[PF_6]$_4$ and **4**[PF_6]$_4$ also exhibits several ligand-centred reductions; in the case of **3**[PF_6]$_4$, these are quasi-reversible, while **4**[PF_6]$_4$ shows a reversible ligand reduction at −0.89 V and two quasi-reversible processes at −1.48 and −1.96 V.

Functionalised N-alkyl derivatives of [Ru(pytpy)$_2$]$^{2+}$: Given the successful preparation and isolation of the N-alkylated complexes **4**$^{4+}$ and **5**$^{4+}$, we turned our attention to N-alkylated derivatives of **2**$^{2+}$ containing pendant functionalities. The strategy for the formation of complexes **5**$^{4+}$, **6**$^{4+}$ and **7**$^{4+}$ was the same as for **3**$^{4+}$ and **4**$^{4+}$. In each case, **2**$^{2+}$ was treated with an alkylating agent in large excess to ensure the formation of the N,N′-dialkylated products. In the case of the preparation of **5**$^{4+}$ and **6**$^{4+}$, the excess of 1,4-bis(bromomethyl)benzene or 1,10-dibromodecane also ensured that reaction occurred at only one of the bromo groups, thus providing complexes **5**$^{4+}$ and **6**$^{4+}$ with pendant electrophilic groups. The reactions of **2**[PF_6]$_2$ with 1,4-bis(bromomethyl)-benzene or 1,10-dibromodecane were significantly slower than with benzyl bromide or 2-bromomethylnaphthalene, and reactions times >48 h were required to achieve complete alkylation. The progress of the reactions was monitored by spot TLC. After only 24 h, two pink products were present; prolonged heating of the reaction mixture in refluxing acetonitrile led to the gradual disappearance of the species with the lower R_f value, and an increase in the amount of the other fraction. We assume that the lower R_f fraction is the monoalkylated derivative of **2**$^{2+}$. After workup, **5**[PF_6]$_4$ and **6**[PF_6]$_4$ were isolated in 35 and 74% yields, respectively.

In the ES mass spectrum of **5**[PF_6]$_4$, no parent ion nor ions with characteristic Br-containing isotopic distributions could be observed. The dominant peak envelopes in the mass spectrum arose from the fragments [Ru(pytpy)$_2$(PF_6)]$^+$ (m/z=867), [Ru(pytpy)$_2$]$^+$ (m/z=720) and [Ru(pytpy)$_2$]$^{2+}$ (m/z=362, base peak). In contrast, the ES mass spectrum of **6**[PF_6]$_4$ exhibited peaks at m/z=1597 and 1451 assigned to [M−PF_6]$^+$ and [M−2PF_6]$^+$, respectively, in addition to the base peak at m/z=362 assigned to [Ru(pytpy)$_2$]$^{2+}$ and a peak at m/z=529 arising from [Br(CH_2)$_{10}$pytpy]$^+$. The isotopic distribution of each peak matched those of the simulated spectrum. The ^{1}H NMR spectrum of **5**[PF_6]$_4$ confirmed the expected molecular symmetry with a single set of signals for the pytpy unit with chemical shifts close to those found for **3**$^{4+}$ and **4**$^{4+}$ (Table 1). In addition, singlets at δ=5.89 and 4.65 ppm were assigned to the NCH_2 and CH_2Br protons, and an AB pattern (δ=9.11 and 8.78 ppm) to the 1,4-phenylene protons. The ^{1}H NMR spectroscopic signature for the pytpy unit in **6**[PF_6]$_4$ was similar to that in **5**[PF_6]$_4$ (Table 1), and signals in the range δ=4.68–≈1.3 ppm were assigned to the (CH_2)$_{10}$Br chain. The ^{13}C NMR spectrum confirmed the symmetry of the system and was fully assigned by using HMQC and HMBC techniques.

Complexes **5**$^{4+}$ and **6**$^{4+}$ possess pendant electrophilic sites and are potential building blocks for metallamacrocyclic or polymeric systems. An alternative strategy that has already been widely exploited[5–28] is to design building blocks that are terminated in metal-binding domains, and we have now coupled this approach with the N-alkylation of **2**$^{2+}$ to generate a new class of functionalised metallasupramolecules. The reaction of **2**[PF_6]$_2$ with an excess of 4′-(4-bromomethylphenyl)-2,2′:6′,2″-terpyridine in CH_3CN under reflux was monitored by spot TLC and was judged to be complete after 64 h; complex **7**[PF_6]$_4$ was isolated as a pink solid. The highest mass peak in the ES mass spectrum came at m/z= 1334 and was assigned to the ion [M−$CH_2C_6H_4$tpy−2PF_6]$^+$; a peak at m/z=632 ([pytpy$CH_2C_6H_4$tpy]$^+$) was also observed. Other dominant peaks in the mass spectrum arose from [Ru(pytpy)$_2$(PF_6)]$^+$ (m/z=867), [Ru(pytpy)$_2$]$^+$ (m/z= 722) and [Ru(pytpy)$_2$]$^{2+}$ (m/z=362, base peak). When recording the ^{1}H NMR spectrum of **7**[PF_6]$_4$, it was necessary to add a small amount of K_2CO_3 to the solution in the NMR tube to prevent protonation of the pendant tpy nitrogen atoms; in the absence of base, only broad resonances, indicative of protonation, were observed. The ^{1}H NMR spectrum confirmed that both pyridine rings in **2**$^{2+}$ had been alkylated, with two tpy environments being apparent, and the signals were assigned from the COSY spectrum. While one set of signals for the tpy protons in **7**$^{4+}$ resembled those for **3**$^{4+}$, **4**$^{4+}$, **5**$^{4+}$ and **6**$^{4+}$, the second set was diagnostic of a non-coordinated tpy ligand; signals for protons H^{3B}, H^{5A} and H^{6A} are significantly perturbed upon coordination (Table 1). The ^{13}C NMR spectrum of **7**[PF_6]$_4$ also clearly indicated the presence of two tpy environments, and the spectrum was fully assigned by using HMQC and HMBC techniques.

In the present work, the conditions for the synthesis of **2**[PF_6]$_2$ varied from those previously reported[30] in that $RuCl_3$·3H_2O and pytpy were heated in ethane-1,2-diol for one rather than three hours. Under these conditions (and after workup), a second product was isolated which was identified as **8**[PF_6]$_4$. Its formation clearly originates from the alkylation of **2**[PF_6]$_2$ by ethane-1,2-diol. Although isolated in only 8% yield, **8**[PF_6]$_4$ represents a further example of a functionalised N-alkyl derivative of [Ru(pytpy)$_2$]$^{2+}$. The FAB mass spectrum of **8**[PF_6]$_4$ exhibited peaks at m/z=1247 ([M−PF_6]$^+$) and 1102 ([M−2PF_6]$^+$). The ^{1}H and ^{13}C NMR spectra of **8**[PF_6]$_4$ were consistent with the formation of a symmetrical product and the spectra were fully assigned by using COSY, HMQC and HMBC methods. The data in Table 1 show that the signals assigned to the pytpy protons appear at chemical shifts close to those of the other N-alkylated derivatives.

The electronic absorption spectra of solutions of **5**[PF_6]$_4$, **6**[PF_6]$_4$, **7**[PF_6]$_4$ and **8**[PF_6]$_4$ in CH_3CN were similar to those of the complexes **3**[PF_6]$_4$ and **4**[PF_6]$_4$. Each complex exhibit-

ed an MLCT absorption in the range 508–512 nm, and a series of intense bands in the UV region assigned to ligand-centred $\pi^*\leftarrow\pi$ transitions. Each complex was redox active and was studied by CV and DPV methods. The complexes **5**$[PF_6]_4$, **6**$[PF_6]_4$, **7**$[PF_6]_4$ and **8**$[PF_6]_4$ exhibited ruthenium-centred oxidations at +1.01, +0.99, +1.01 and +1.02 V, respectively, showing little variation from the behaviour of the model complexes. Each complex exhibited a series of ligand-based reduction processes, which were typically quasi-reversible or irreversible.

Metallamacrocycle formation: The ready N-alkylation of $\mathbf{1}^{2+}$ [44] and $\mathbf{2}^{2+}$ led us to apply this strategy to the formation of iron(II) and ruthenium(II)-containing metallamacrocyclic complexes by reaction with bis(alkylating) reagents. By analogy with the reactions of $\mathbf{1}^{2+}$ and $\mathbf{2}^{2+}$ with benzyl bromide, we chose the dibromo derivatives **9** and **10** to react with $\mathbf{1}^{2+}$ and $\mathbf{2}^{2+}$ in the hope of forming [2+2] metallamacrocycles.

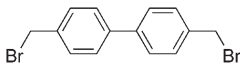

9

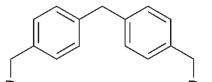

10

Initially, we attempted a one-step assembly process by the direct reaction of $\mathbf{1}^{2+}$ with **9** in refluxing CH_3CN. Complex **1**$[PF_6]_2$ was added to a solution of **9** over a six hour period and then heating was continued for a further 72 hours. When the resulting dark blue solution was analysed by TLC, one major blue component was observed and was shown (see below) to be **11**$[PF_6]_6$ (Scheme 1). Chromatographic separation of the reaction mixture led to the isolation of several minor fractions, but none proved to be the target [2+2] macrocyclic product. By using a 2:1 molar ratio of $\mathbf{1}^{2+}$/**9** in the reaction, **11**$[PF_6]_6$ could be isolated in 23% yield. The ^{1}H NMR spectrum of **11**$[PF_6]_6$ (assigned by using COSY and NOESY techniques) confirmed the presence of two different coordinated tpy environments. Signals for the pendant pyridine protons also indicated two different environments, one N-alkylated and one not.[30] Electrochemical studies showed that **11**$[PF_6]_6$ exhibits one iron-centred oxidation process at +0.79 V, and a second process at +1.04 V, the origin of which we have not elucidated. Reduction processes are dominated by an absorption peak at $\approx$ −1.2 V.

Attempts to react **11**$[PF_6]_6$ with another equivalent of **9** in order to achieve the desired [2+2] metallamacrocyclic complex were unsuccessful. We therefore turned to the alternative strategy outlined in Scheme 2 involving alkylation of the free pytpy ligand. The reaction between pytpy and either **9** or **10** in CH_3CN at reflux followed by precipitation of the products as hexafluorophosphate salts, resulted in the formation of **12**$[PF_6]_2$ or **13**$[PF_6]_2$ in 62 and 55% yields, respectively. Solvent choice is important; attempts to prepare **12**$[PF_6]_2$ in EtOH, *i*PrOH or DMF resulted in yields of 0, 28 or 37%, respectively. The MALDI-TOF mass spectra of **12**$[PF_6]_2$ and **13**$[PF_6]_2$ each showed a peak assigned to $[M-PF_6]^+$ (m/z = 947 and 959, respectively). The ^{1}H NMR spectra of the two compounds were similar, with the exception of the alkyl region. For **12**$[PF_6]_2$, this exhibited a singlet

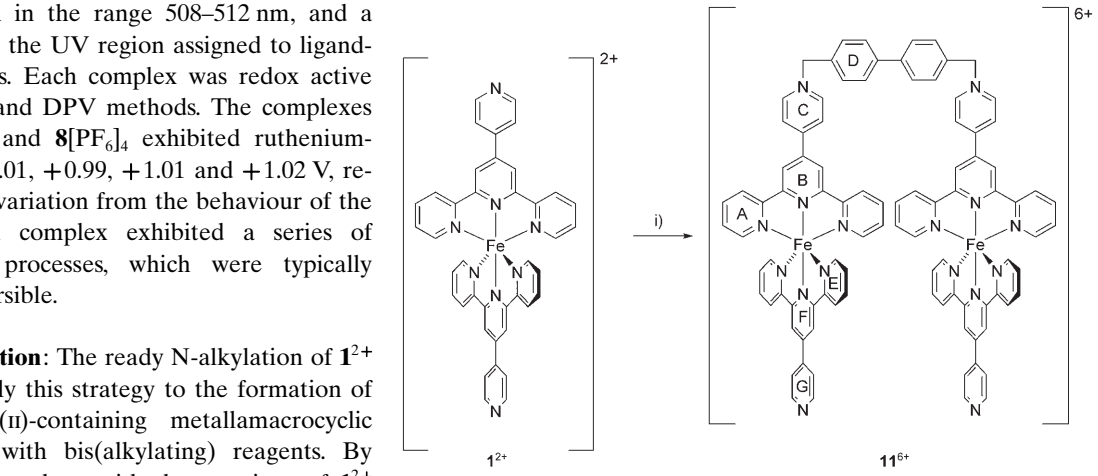

$\mathbf{1}^{2+}$ $\mathbf{11}^{6+}$

Scheme 1. The 1:1 reaction of $\mathbf{1}^{2+}$ and **9**: i) **9**, CH_3CN, reflux. The ring labelling is that used for NMR spectroscopic assignments.

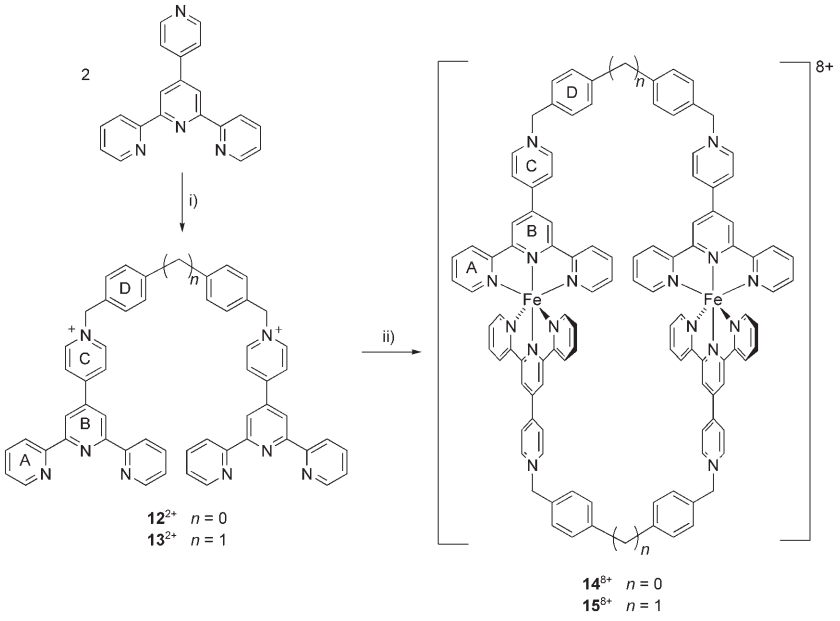

$\mathbf{12}^{2+}$ $n = 0$
$\mathbf{13}^{2+}$ $n = 1$

$\mathbf{14}^{8+}$ $n = 0$
$\mathbf{15}^{8+}$ $n = 1$

Scheme 2. Reaction steps for the formation of [2+2] iron-containing macrocyclic complexes: i) **9** or **10**, CH_3CN, reflux; ii) $Fe(BF_4)_2{\cdot}6H_2O$, CH_3CN/CH_3OH. The ring labelling is that used for NMR spectroscopic assignments.

at $\delta = 5.83$ ppm for the NCH_2, while **13**$[PF_6]_2$ showed two singlets at $\delta = 5.72$ and 4.04 ppm (relative integrals 2:1) assigned to NCH_2 and the CH_2 group between the D rings (Scheme 2), respectively. A single set of tpy proton signals for each compound confirmed the expected molecular symmetry. The assignment of the pyridine protons H^{C2} and H^{C3} was made by NOE experiments.

The N-alkylated species $\mathbf{12}^{2+}$ or $\mathbf{13}^{2+}$ are sufficiently flexible bis(tpy) ligands to enable the formation of metallamacrocycles when treated with iron(II). Since competitive polymer formation was expected, reactions were carried out at high dilution to optimise the formation of metallamacrocyclic products. Solutions of **12**$[PF_6]_2$ or **13**$[PF_6]_2$ ($\approx 10^{-4}$ mol dm^{-3} in CH_3CN) and $Fe(BF_4)_2 \cdot 6H_2O$ ($\approx 10^{-4}$ mol dm^{-3} in CH_3CN) were added simultaneously to a stirred mixture of CH_3CN and CH_3OH (1:1) over a period of four days at room temperature. The solution developed a blue colour, which deepened during the reaction period. Attempts to separate the products by chromatography on silica led to decomposition, and fractional precipitation was used to separate **14**$[PF_6]_8$ and **15**$[PF_6]_8$ from residual precursors and any polymeric material. Initially, all complexes in the reaction mixture were precipitated as hexafluorophosphate salts by adding aqueous NH_4PF_6. These salts were dissolved in CH_3CN and a few drops of saturated aqueous KNO_3 were added causing a deep blue precipitate to form. Analysis by thin-layer chromatography revealed this material to be intractable and it was therefore assumed to be polymeric. Dropwise addition of further saturated aqueous KNO_3 to the filtrate led to additional precipitate. Again, this was analysed by TLC, and the process was repeated until a blue precipitate that was mobile on silica was obtained. Careful repetition of this process resulted in **14**$[PF_6]_8$ and **15**$[PF_6]_8$ being collected in 35 and 16% yields, respectively.

The highest mass peak in the ES mass spectrum of **14**$[PF_6]_8$ appeared at m/z 1291 and was assigned to the fragment $[M-2PF_6]^{2+}$. Loss of further PF_6^- led to a series of peaks at $m/z = 813$ ($[M-3PF_6]^{3+}$), 573 ($[M-4PF_6]^{4+}$), 430 ($[M-5PF_6]^{5+}$, the base peak) and 334 ($[M-6PF_6]^{6+}$). In the ES spectrum of **15**$[PF_6]_8$, peaks at $m/z = 822$ ($[M-3PF_6]^{3+}$) and 580 ($[M-4PF_6]^{4+}$) were observed in addition to a relatively intense peak at $m/z = 338$ ($[Fe(pytpy)_2]^{2+}$). The base peak at $m/z = 407$ and an intense peak at $m/z = 959$ were assigned to $\mathbf{13}^{2+}$ and $[\mathbf{13}+PF_6]^+$, respectively.

The solution ^{1}H NMR spectra of **14**$[PF_6]_8$ and **15**$[PF_6]_8$ confirmed the formation of a symmetrical products. All proton signals were fully assigned by standard techniques. The shift of signals assigned to protons H^{6A} (from $\delta = 8.91$ to 7.01 ppm) and H^{3B} (from $\delta = 8.88$ to 9.16 ppm) on going from **12**$[PF_6]_2$ to **14**$[PF_6]_8$ confirmed coordination of the tpy domains to iron(II). Similar shifts were observed on forming **15**$[PF_6]_8$. We have previously pointed to the fact that protons H^{4A} and H^{5A} are diagnostic probes for metallamacrocyclic complex versus metallapolymer formation.[21] On going from ligand $\mathbf{12}^{2+}$ to complex $\mathbf{14}^{8+}$, the shift difference $\{\delta(\text{ligand})-\delta(\text{complex})\}$ is $+0.21$ ppm for H^{4A} and $+0.56$ ppm for H^{5A} (both in CD_3CN). These are consistent with the formation of a macrocyclic complex. Significantly greater values for $\{\delta(\text{ligand})-\delta(\text{complex})\}$ of $+0.52$ ppm for H^{4A} and $+0.92$ ppm for H^{5A} are observed on going from ligand $\mathbf{13}^{2+}$ to complex $\mathbf{15}^{8+}$ (both in CD_3CN). The origin of this increased shift to lower frequency can be traced to the change in shape of the macrocyclic cavity when the additional CH_2 groups are introduced into the backbone of ligand on going from $\mathbf{12}^{2+}$ to $\mathbf{13}^{2+}$. Figure 2 shows modelled structures of $\mathbf{14}^{8+}$ and $\mathbf{15}^{8+}$, and illustrates the elongation of the cavity. The modelled structures suggest that two pyridine rings face each other across the macrocyclic cavity, elongation of which results in the pyridine rings coming closer together and the evolution of possible π-stacking interactions. The pyridine ring centroid–-centroid distances are ≈7.5 Å in $\mathbf{14}^{8+}$, and ≈3.6 Å in $\mathbf{15}^{8+}$. The presence of a through-space interaction between protons H^{3A} and H^{6A} of different $\{Fe(tpy)_2\}$ units in **14**$[PF_6]_8$ and in **15**$[PF_6]_8$ was confirmed by ROESY experiments. The room-temperature solution ^{1}H NMR spectrum of each of **14**$[PF_6]_8$ and **15**$[PF_6]_8$ showed that the two terminal pyridine rings of each tpy unit were equivalent and indicated that there was rotation of each $\{Fe(tpy)_2\}$ unit on the NMR timescale. Variable-temperature ^{1}H NMR spectra of solutions of **14**$[PF_6]_8$ and **15**$[PF_6]_8$ in acetonitrile were recorded over a temperature range of 295–228 K. Apart from some broadening of the signals and slight shifting to lower frequency, no significant changes were observed.

Both iron(II) macrocyclic complexes were electrochemically active. Complexes **14**$[PF_6]_8$ and **15**$[PF_6]_8$ exhibit iron-centred oxidation processes at $+0.85$ and $+0.86$ V, respectively. These potentials are similar to those reported for N-alkylated derivatives of $[Fe(pytpy)_2]^{2+}$.[44] Only one Fe^{2+}/Fe^{3+} process was observed for each diiron complex. Ligand-centred reductive processes were observed at -1.09, -1.47 and -1.76 V for **14**$[PF_6]_8$, and at -1.07, -1.33 and -1.77 V for **15**$[PF_6]_8$. All are quasi-reversible or irreversible, and the peaks for the most negative processes in the cyclic voltammograms were poorly resolved.

Attempts to prepare $\mathbf{16}^{8+}$ in a two-step process involving double N-alkylation of $\mathbf{2}^{2+}$ with two equivalents of **10** followed by ring closure by treatment with a second equivalent of $\mathbf{2}^{2+}$ were unsuccessful. Although our efforts to prepare $\mathbf{14}^{2+}$ by reaction of $\mathbf{2}^{2+}$ with an equimolar amount of **9** had failed, this strategy proved to be the most efficient for the formation of the related ruthenium(II) macrocyclic complex $\mathbf{16}^{8+}$ (Scheme 3). Equimolar amounts of the dibromo derivative **10** and **2**$[PF_6]_2$ were heated at reflux in CH_3CN (concentration $\approx 10^{-2}$ mol dm^{-3}) and the reaction was monitored by TLC. Two pink products in addition to the red starting material were observed after several hours, and a third pink material ($R_F = 0.1$) appeared after 24 h. Over the next 72 h, the last product became the predominant component of the reaction mixture, and only traces of the initial two pink products remained. After workup, **16**$[PF_6]_8$ was isolated in 29% yield. The highest mass peak in the MALDI-TOF mass spectrum of **16**$[PF_6]_8$ was observed at $m/z = 2701$ ($[M-2PF_6]^+$), and the base peak ($m/z = 722$) arose from the

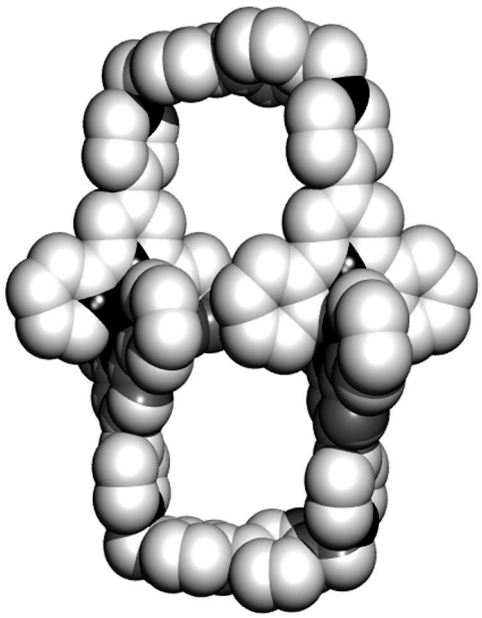

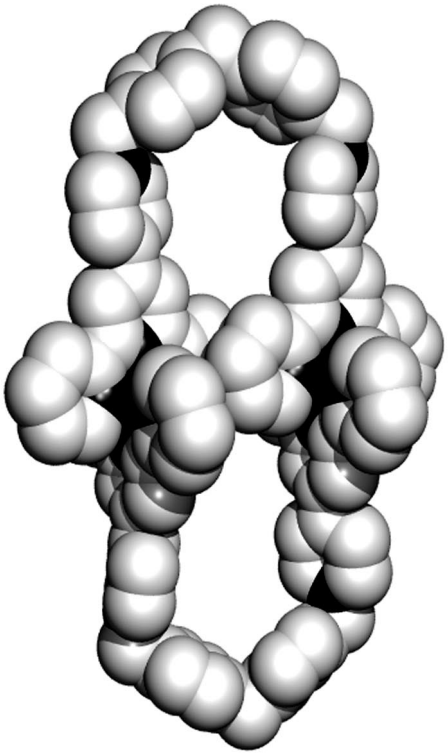

Figure 2. Space-filling models of $\mathbf{14}^{8+}$ (top) and $\mathbf{15}^{8+}$ (bottom) illustrating the difference in the shape of the macrocyclic cavity which allows the $\{Fe(tpy)_2\}$ units to approach more closely.

fragment $[Ru(pytpy)_2]^+$. The solution ^1H and ^{13}C NMR spectra of the complex were fully assigned by using COSY, HMQC and HMBC techniques, and confirmed the formation of a symmetrical species. The appearance of the signals assigned to protons H^{4A} and H^{5A} at $\delta = 7.54$ and 6.63 ppm, respectively, was diagnostic (as discussed above for $\mathbf{14}^{8+}$ and

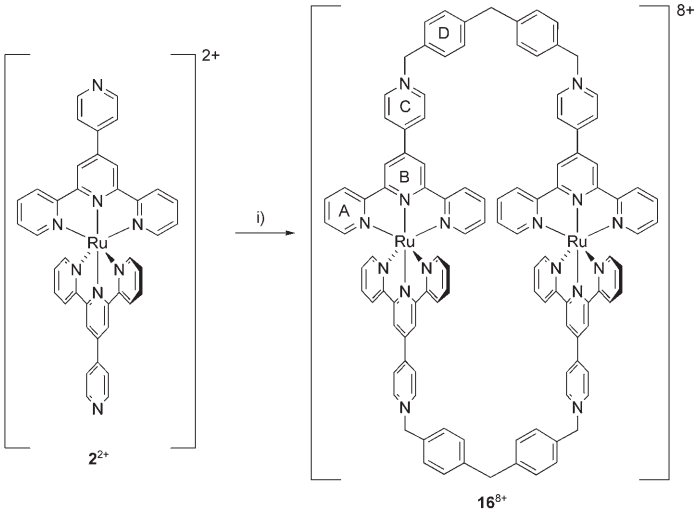

Scheme 3. Strategy for the formation of [2+2] ruthenium-containing macrocycle: i) **10**, CH_3CN, reflux. The ring labelling is that used for NMR spectroscopic assignments.

$\mathbf{15}^{8+}$) of the formation of a cyclic rather than acyclic system. The presence of a single set of signals for the outer rings of the tpy ligands indicated that the $\{Ru(tpy)_2\}$ units undergo rotation on the NMR spectroscopic timescale. The electronic absorption spectrum of a solution of $\mathbf{16}[PF_6]_8$ in acetonitrile was similar to those of the N-alkylated ruthenium(II) complexes described above. An MLCT absorption was observed at 507 nm, and intense bands in the UV region were assigned to ligand-centred $\pi^* \leftarrow \pi$ transitions. The complex $\mathbf{16}[PF_6]_8$ was electrochemically active. CV and DPV studies revealed a single metal-centred oxidation process at +1.06 V, which is reminiscent of the mononuclear ruthenium(II) N-alkylated complexes discussed earlier. Three ligand-centred reduction processes were observed at −1.03 V (reversible reduction), −1.48 V (quasi-reversible reduction) and −1.65 V (irreversible reduction).

Conclusion

We have prepared and characterised a series of N-alkylated derivatives of $[Ru(pytpy)_2]^{2+}$ ($\mathbf{2}^{2+}$), which includes both model and functionalised complexes. The results have allowed a comparison with analogous iron(II) species, and illustrate that the $[M(pytpy)_2]^{2+}$ (M = Fe, Ru) complex has the potential to be used as a building block for the formation of metallamacrocyclic complexes through N-alkylation at the pendant pyridine rings. However, it has been shown that a single synthetic approach cannot be used to form both iron(II) and ruthenium(II) [2+2] metallamacrocycles. Whereas treatment of $\mathbf{2}^{2+}$ with the dibromo derivative **10** leads to the formation of $\mathbf{16}^{8+}$ in moderate yield, related iron(II) macrocycles could not be accessed by this route. A two-step route involving the initial formation of ditopic ligands $\mathbf{12}^{2+}$ and $\mathbf{13}^{2+}$ followed by treatment with iron(II) was found to be the most efficient means of generating macrocy-

cles $\mathbf{14}^{8+}$ and $\mathbf{15}^{8+}$. In each dinuclear complex, electrochemical studies provide no evidence for electronic communication between the metal centres.

Experimental Section

General methods: Infrared spectra were recorded on a Mattson Genesis Fourier transform spectrophotometer with samples in compressed KBr discs or on a FTIR-8400S spectrophotometer with samples as solids using a Golden Gate ATR accessory. ^{1}H and ^{13}C NMR spectra were recorded on Bruker AM250, DRX500 or DRX600 MHz spectrometers; the numbering scheme adopted for the ligands is shown in the structure diagrams, and chemical shifts are referenced with respect to TMS $\delta = 0$ ppm. UV/Vis measurements were recorded on a Varian Cary 5000 UV/Vis/NIR spectrophotometer in acetonitrile. Electrospray mass spectra (ESMS) were recorded on a Finnigan MAT LCQ ESI/MS instrument. MALDI-TOF mass spectra were recorded on a PerSeptive Biosystems Voyager DEPRO Biospectrometry Workstation. Elemental analyses were carried out in the Department of Chemistry, University of Basel, at CMAS Microanalytical Services, Melbourne, or at the Campbell Microanalytical Laboratory, University of Otago. Electrochemical measurements were performed with an Eco Chemie Autolab PGSTAT 20 system using glassy carbon (except for $\mathbf{5}[PF_6]_4$) or platinum (for $\mathbf{5}[PF_6]_4$) working and platinum auxiliary electrodes with a silver wire as quasi-reference; the working electrode was polished with aluminium oxide powder (0.3 micrometer) before use; purified CH_3CN (Fluka) was used as solvent and 0.1 M $[n\mathrm{Bu}_4\mathrm{N}][BF_4]$ as supporting electrolyte. Potentials are quoted versus the ferrocene/ferrocenium couple ($Fc/Fc^+ = 0.0$ V), and all potentials were referenced to internal ferrocene added at the end of each experiment. The compounds pytpy,[29] $[Fe(pytpy)_2]^{2+}$ salts,[29] **9**,[54] **10**[55,56] and 4′-(4-methylphenyl)-2,2′:6′,2″-terpyridine[57] were prepared by literature methods. All solvents were freshly distilled and reactions were carried out under N_2.

Complexes $\mathbf{2}[PF_6]_2$ and $\mathbf{8}[PF_6]_4$: The literature method[30] was followed but with a heating time of 1 h instead of 3 h. Reaction scale: $RuCl_3\cdot 3H_2O$ (19 mg, 0.079 mmol) and pytpy (49 mg, 0.16 mmol) in ethane-1,2-diol (10 cm^3). Column chromatographic workup (silica, CH_3CN/saturated aqueous KNO_3/water 7:1:0.5) gave two fractions. The major red fraction was collected and volume of solvent was reduced; $\mathbf{2}[PF_6]_2$ (54 mg, 68%) was precipitated by addition of saturated methanolic solution of NH_4PF_6. Spectroscopic data were identical with those reported.[30] A pink fraction with lower R_f value than the major product was also collected and was identified as $[\mathbf{8}][PF_6]_4$ (9 mg, 8%). FAB-MS: m/z: 1247 $[M-PF_6]^+$, 1102 $[M-2PF_6]^+$; ^{1}H NMR (500 MHz, CD_3CN): $\delta = 9.15$ (s, 4H; H^{3B}), 9.03 (d(AB), $J = 7.0$ Hz, 4H; H^{2C}), 8.76 (d(AB), $J = 6.5$ Hz, 4H; H^{3C}), 8.69 (d, $J = 8.0$ Hz, 4H; H^{3A}), 8.01 (dt, $J = 8.0$, 1.5 Hz, 4H; H^{4A}), 7.44 (d, $J = 5.6$, 1.4, 0.7 Hz, 4H; H^{6A}), 7.24 (ddd, $J = 7.5$, 5.7, 1.3 Hz, 4H; H^{5A}), 4.77 (t, $J = 5.0$ Hz, 4H; CH_2), 4.10 (br t, 4H; OCH_2), 3.60 ppm (br s, 2H; OH); ^{13}C NMR (125 MHz, CD_3CN): $\delta = 158.3$ (C^{2A}), 156.8 (C^{2B}), 153.7 ($C^{4B/4C}$), 153.6 (C^{6A}), 146.8 (C^{2C}), 142.1 ($C^{4C/4B}$), 139.5 (C^{4A}), 128.9 (C^{5A}), 127.0 (C^{3C}), 125.9 (C^{3A}), 123.3 (C^{3B}), 64.7 ($C_{OCH_2CH_2}$), 61.2 ppm (C^{OCH_2}); UV/Vis (CH_3CN): λ_{max} (ε) = 246 (40.9×10^3), 274 (90.3×10^3), 310 (38.2×10^3), 338 (50.2×10^3), 508 nm (48.3×10^3 dm^{3}mol^{-1}cm^{-1}); IR (solid): $\tilde{\nu} = 3579$ (w), 3084 (w), 1644 (s), 1605 (m), 1535 (m), 1467 (m), 1424 (s), 1398 (m), 1355 (m), 1246 (w), 1174 (w), 1025 (m), 780 (vs), 751 (vs), 742 cm^{-1} (s); elemental analysis calcd (%) for $C_{44}H_{38}F_{24}N_8O_2P_4Ru\cdot CH_3CN\cdot H_2O$: C 38.1, H 3.0, N 8.7; found: C 38.2, H 3.6, 8.6; E° (vs. Fc/Fc^+) = +1.02, −0.89 (reversible reduction), −1.48 (quasi-reversible reduction), −1.96 V (irreversible reduction).

Complex $\mathbf{3}[PF_6]_4$: Complex $\mathbf{2}[PF_6]_2$ (21 mg, 0.020 mmol) was dissolved in CH_3CN (25 cm^3) and benzyl bromide (1.0 cm^3, 8.4 mmol) was added. The red solution was heated under reflux for 2 h, after which TLC analysis (silica, CH_3CN/saturated aqueous KNO_3/water 7:1:0.5) revealed the disappearance of all starting material and formation of a single pink product. After evaporating the solvent, a saturated methanolic solution (5 cm^3) of NH_4PF_6 was added to the mixture of crude product and excess alkylating agent, and a red solid precipitated. This was filtered through Celite and washed with methanol (5 cm^3), and then water (20 cm^3). The solid was dried in air, and then removed from the Celite by dissolution in CH_3CN. After removal of solvent, $\mathbf{3}[PF_6]_4$ was collected; a small amount of residual benzyl bromide (shown by ^{1}H NMR spectroscopy) was removed by washing with Et_2O (3×5 cm^3) and decanting the supernatant solution. Yield 24 mg, 68%; ES-MS: m/z: 1339 $[M-PF_6]^+$, 597 $[M-2PF_6]^{2+}$, 362 $[Ru(pytpy)_2]^{2+}$; ^{1}H NMR (500 MHz, CD_3CN): $\delta = 9.14$ (s, 4H; H^{3B}), 9.09 (d(AB), $J = 7.0$ Hz, 4H; H^{2C}), 8.77 (d(AB), $J = 7.0$ Hz, 4H; H^{3C}), 8.70 (ddd, $J = 8.3$, 1.5, 0.8, 4H; H^{3A}), 8.00 (dt, $J = 7.8$, 1.5 Hz, 4H; H^{4A}), 7.58 (m, 10H; H^D), 7.43 (ddd, $J = 5.5$, 1.5, 0.5 Hz, 4H; H^{6A}), 7.23 (ddd, $J = 7.5$, 5.5, 1.5 Hz, 4H; H^{5A}), 5.91 ppm (s, 4H; CH_2); ^{13}C NMR (125 MHz, CD_3CN): $\delta = 158.4$ (C^{2A}), 157.0 (C^{2B}), 154.2 ($C^{4B/4C}$), 153.7 (C^{6A}), 146.4 (C^{2C}), 142.1 ($C^{4C/4B}$), 139.7 (C^{4A}), 133.9 (C^{1D}), 131.2 (C^{4D}), 130.7 ($C^{2D/3D}$), 130.4 ($C^{3D/2D}$), 129.1 (C^{5A}), 127.8 (C^{3C}), 126.1 (C^{3A}), 123.4 (C^{3B}), 65.6 ppm (C_{CH_2}); UV/Vis (CH_3CN): λ_{max} (ε) = 241 (48.2×10^3), 277 (74.1×10^3), 312 (31.5×10^3), 341 (34.3×10^3), 511 nm (35.9×10^3 dm^{3}mol^{-1}cm^{-1}); IR (solid): $\tilde{\nu} = 3507$ (w), 3399 (w), 3072 (w), 1664 (s), 1636 (s), 1524 (m), 1457 (m), 1423 (s), 1410 (m), 1355 (m), 1292 (m), 1249 (w), 1164 (m), 1091 (w), 1029 (m), 817 (vs), 793 (vs), 787 (vs), 740 (vs), 732 cm^{-1} (s); elemental analysis calcd (%) for $C_{54}H_{42}F_{24}N_8P_4Ru\cdot CH_3CN$: C 44.1, H 3.0, N 8.3; found: C 44.0, H 2.9, 8.3; E° (vs. Fc/Fc^+): +1.01, −0.98, −1.24, −1.52, −1.89 V (quasi-reversible reductions).

Complex $\mathbf{4}[PF_6]_4$: Complex $\mathbf{2}[PF_6]_2$ (20 mg, 0.020 mmol) and 2-bromomethylnaphthalene (18 mg, 0.081 mmol) was dissolved in CH_3CN (20 cm^3), and the solution was heated to reflux. After 24 h, heating was stopped and a red precipitate was observed. Water (1 cm^3) was added and the precipitate dissolved. The solution was concentrated in volume to 5 cm^3, and saturated aqueous NH_4PF_6 was added to precipitate the product. However, the residue formed an oil. $CHCl_3$ (5 cm^3) was added in an attempt to remove excess alkylating agent, but no solid product could be obtained from the biphasic mixture. The chloroform, excess CH_3CN and some water were removed by evaporation, causing the oil to form a dark pink solid. This was filtered through Celite and washed with water (50 cm^3) and $CHCl_3$ (30 cm^3) to remove excess 2-bromomethylnaphthalene. The solid was dried in air, and then removed from the Celite by dissolution in CH_3CN. Solvent was removed, and the crude product was purified by column chromatography (silica, CH_3CN/saturated aqueous KNO_3/water 7:1:0.5). The major pink fraction was collected, evaporated and reprecipitated with NH_4PF_6 solution to afford $[\mathbf{4}][PF_6]_4$. Yield 22 mg, 71%; ES-MS: m/z: 1439 $[M-PF_6]^+$, 1294 $[M-2PF_6]^+$, 1152 $[M-(\mathrm{napCH_2})-2PF_6]^+$, 867 $[Ru(pytpy)_2(PF_6)]^+$, 722 $[Ru(pytpy)_2]^+$, 362 $[Ru(pytpy)_2]^{2+}$; ^{1}H NMR (500 MHz, CD_3CN): $\delta = 9.19$ (s, 4H; H^{3B}), 9.18 (d(AB), $J = 6.9$ Hz, 4H; H^{2C}), 8.83 (d(AB), $J = 6.9$ Hz, 4H; H^{3C}), 8.72 (d, $J = 8.0$ Hz, 4H; H^{3A}), 8.17 (s, 2H; H^{1D}), 8.07 (d, $J = 8.5$, 2H; H^{4D}), 8.01 (m, 4H; $H^{5D,8D}$), 7.99 (dt, $J = 7.9$, 1.3 Hz, 4H; H^{4A}), 7.66 (m, 6H; $H^{3D,6D,7D}$), 7.43 (dd, $J = 5.7$, 1.3 Hz, 4H; H^{6A}), 7.22 (ddd, $J = 7.4$, 5.6, 1.2 Hz, 4H; H^{5A}), 6.07 ppm (s, 4H; CH_2); ^{13}C NMR (125 MHz, CD_3CN): $\delta = 158.3$ (C^{2A}), 156.8 (C^{2B}), 154.0 ($C^{4B/4C}$), 153.6 (C^{6A}), 146.5 (C^{2C}), 141.9 ($C^{4C/4B}$), 139.5 (C^{4A}), 134.5 ($C^{4aD/8aD}$), 134.2 ($C^{8aD/4aD}$), 131.2 (C^{2D}), 130.5 ($C^{1D/4D}$), 130.4 ($C^{4D/1D}$), 129.1 ($C^{5D/8D}$), 128.9 (C^{5A}), 128.8 ($C^{8D/5D}$), 128.5 ($C^{6D/7D}$), 128.2 ($C^{7D/6D}$), 127.6 (C^{3C}), 126.7 (C^{3D}), 126.0 (C^{3A}), 123.3 (C^{3B}), 65.5 ppm (C_{CH_2}); UV/Vis (CH_3CN): λ_{max} (ε) = 224 (114.5×10^3), 277 (57.7×10^3), 341 (23.3×10^3), 513 nm (23.0×10^3 dm^{3}mol^{-1}cm^{-1}); IR (solid): $\tilde{\nu} =$ 3400 (w), 3063 (w), 1668 (w), 1636 (s), 1603 (m), 1525 (w), 1422 (m), 1338 (s), 1331 (s), 1293 (m), 1248 (m), 1160 (m), 1091 (w), 1029 (m), 823 (vs), 786 (vs), 754 cm^{-1} (vs), elemental analysis calcd (%) for $C_{62}H_{46}F_{24}N_8P_4Ru\cdot 3CH_3CN\cdot 3H_2O$: C 46.4, H 3.5, N 8.8; found: C 46.4, H 3.2, N 9.2; E° (vs. Fc/Fc^+): +1.01, −1.21, −1.47 V (quasi-reversible reductions).

Complex $\mathbf{5}[PF_6]_4$: Complex $\mathbf{2}[PF_6]_2$ (21 mg, 0.020 mmol) and 1,4-bis(bromomethyl)benzene (16 mg, 0.061 mmol) were dissolved in CH_3CN (25 cm^3) and the mixture heated at reflux for 72 h. The solution was then concentrated in vacuo to ≈5 cm^3, and saturated aqueous solution of NH_4PF_6 was added to precipitate the crude product. The solid was filtered through Celite and washed with water (20 cm^3), and $CHCl_3$ (20 cm^3) to remove excess 1,4-bis(bromomethyl)benzene. Purification of the product by column chromatography (silica, CH_3CN/saturated aque-

ous KNO_3/water 7:1:0.5) and precipitation with aqueous NH_4PF_6 afforded **5**$[PF_6]_4$ as a dark pink solid (12 mg, 35%). Crystalline material suitable for microanalysis was obtained by diffusion of Et_2O vapour into a solution of **5**$[PF_6]_4$ in CH_3CN. MALDI-TOF: m/z: 867 $[Ru(pytpy)_2(PF_6)]^+$, 720 $[Ru(pytpy)_2]^+$, 362 $[Ru(pytpy)_2]^{2+}$; ^{1}H NMR (250 MHz, CD_3CN): $\delta=$ 9.16 (s, 4H; H^{3B}), 9.11 (d(AB), $J=6.8$ Hz, 4H; H^{2C}), 8.78 (d(AB), $J=$ 7.0 Hz, 4H; H^{3C}), 8.70 (d, $J=8.0$ Hz, 4H; H^{3A}), 8.00 (dt, $J=8.0$, 1.4 Hz, 4H; H^{4A}), 7.60 (m, 8H; H^{D}), 7.43 (dd, $J=5.3$, 0.8 Hz, 4H; H^{6A}), 7.22 (ddd, $J=7.7$, 5.7, 1.1 Hz, 4H; H^{5A}), 5.89 (s, 4H; NCH_2), 4.65 ppm (s, 4H; CH_2Br); UV/Vis (CH_3CN): $\lambda_{max}=238$, 274, 309, 337, 512; elemental analysis calcd (%) for $C_{56}H_{44}Br_2F_{24}N_8P_4Ru\cdot CH_3CN\cdot H_2O$: C 39.9, H 2.9, N 7.2; found: C 39.5, H 2.9, N 7.2; E° (vs. Fc/Fc^+): +1.01, −0.91, −1.61 V (irreversible reductions).

Complex 6$[PF_6]_4$: Complex **2**$[PF_6]_2$ (42 mg, 0.042 mmol) and 1,10-dibromodecane (0.50 cm^3, 2.2 mmol) were dissolved in CH_3CN (30 cm^3) and the mixture was heated at reflux for 24 h. Additional 1,10-dibromodecane (0.50 cm^3, 2.2 mmol) was then added and heating was continued for a further 30 h. Solvent was then evaporated and the residue triturated with chloroform (5 cm^3) to give a red precipitate. The solid was filtered through Celite and was washed with chloroform (30 cm^3) to remove excess 1,10-dibromodecane. Aqueous CH_3CN (1:1) was used to wash the crude product from the Celite, and the red solution was concentrated in volume to ≈5 cm^3. Addition of saturated aqueous NH_4PF_6 resulted in precipitation of the crude product. This was collected by filtration and purified by column chromatography (silica, CH_3CN/saturated aqueous KNO_3/water 7:1:0.5). The major red fraction was collected, and **6**$[PF_6]_4$ was precipitated from solution as a red solid on addition of saturated aqueous NH_4PF_6. Yield 54 mg, 74%; ES-MS: m/z: 1597 $[M-PF_6]^+$, 1451 $[M-2PF_6]^+$, 529 $[Br(CH_2)_{10}pytpy]^+$, 362 $[Ru(pytpy)_2]^{2+}$; ^{1}H NMR (500 MHz, CD_3CN): $\delta=9.19$ (s, 4H; H^{3B}), 9.04 (d(AB), $J=7.0$ Hz, 4H; H^{2C}), 8.78 (d(AB), $J=6.8$ Hz, 4H; H^{3C}), 8.72 (d, $J=8.0$ Hz, 4H; H^{3A}), 8.01 (dt, 8.0, 1.3 Hz, 4H; H^{4A}), 7.45 (dd, $J=5.4$, 0.8 Hz, 4H; H^{6A}), 7.23 (ddd, $J=7.5$, 5.7, 1.1 Hz, 4H; H^{5A}), 4.68 (t, $J=7.5$ Hz, 4H; NCH_2), 3.48 (t, $J=6.8$ Hz, 4H; CH_2Br), 2.11 (quintet, $J=7.2$ Hz, 4H; NCH_2CH_2), 1.84 (quintet, $J=7.0$ Hz, 4H; CH_2CH_2Br), 1.3–1.5 ppm (overlapping m, 24H; CH_2); ^{13}C (125 MHz, CD_3CN): $\delta=158.3$ (C^{2A}), 156.9 (C^{2B}), 153.6 (C^{6A}), 153.4 ($C^{4C/4B}$), 146.2 (C^{2C}), 141.9 ($C^{4C/4B}$), 139.5 (C^{4A}), 128.9 (C^{5A}), 127.4 (C^{3C}), 126.0 (C^{3A}), 123.2 (C^{3B}), 62.7 (C_{NCH_2}), 35.4 (C_{CH_2Br}), 33.5 (C_{CH_2}), 31.8 ($C_{NCH_2CH_2}$), 29.9 (C_{CH_2}), 29.5 (C_{CH_2}), 29.3 (C_{CH_2}), 28.7 (C_{CH_2}), 26.6 (C_{CH_2}), 22.4 ($C_{CH_2CH_2Br}$); UV/Vis (CH_3CN): λ_{max} (ε) = 276 (96.9×10^3), 305 (48.0×10^3), 340 (39.7×10^3), 509 nm (31.9×10^3 $dm^3mol^{-1}cm^{-1}$); IR (solid): $\tilde{\nu}=3075$ (w), 2925 (m), 2853 (m), 1663 (m), 1640 (s), 1604 (m), 1527 (m), 1484 (w), 1467 (w), 1423 (s), 1360 (m), 1293 (w), 1248 (w), 1175 (m), 1030 (m), 820 (vs), 788 cm^{-1} (vs); elemental analysis calcd (%) for $C_{60}H_{68}N_8Br_2RuP_4F_{24}\cdot2H_2O$ C 40.5, H 4.0, N 6.3; found: C 40.5, H 4.0, N 6.5; E (vs. Fc/Fc^+): +0.99, −1.02, −1.58, −1.90 V (irreversible reductions, poorly resolved).

4′-(4-Bromomethylphenyl)-2,2′:6′,2″-terpyridine: This was prepared by a route modified from that reported by Calzaferri.[57] 4′-(4-Methylphenyl)-2,2′:6′,2″-terpyridine (0.65 g, 2.0 mmol) and *N*-bromosuccinimide (0.37 g, 2.1 mmol) were dissolved in benzene (60 cm^3). Dibenzoyl peroxide (≈20 mg) was added, and the reaction mixture heated under reflux for 42 h. After cooling to room temperature, the suspension was filtered and the solution was washed with water (2×20 cm^3), dried over Na_2SO_4 and the solvent removed under reduced pressure. Recrystallisation of the brown solid from EtOH/acetone (2:1) gave 4′-(4-Bromomethylphenyl)-2,2′:6′,2″-terpyridine as white needles, which were collected by filtration and washed with a small amount of cold 95% EtOH. Yield 377 mg, 47%; spectroscopic data were identical to those in the literature.[57–59]

Complex 7$[PF_6]_4$: Complex **2**$[PF_6]_2$ (21 mg, 0.020 mmol) and 4′-(4-bromomethylphenyl)-2,2′:6′,2″-terpyridine (17 mg, 0.42 mmol) were dissolved in CH_3CN (20 cm^3), and the red solution was heated under reflux for 48 h, followed by addition of more 4′-(4-bromomethylphenyl)-2,2′:6′,2″-terpyridine (8 mg, 0.2 mmol); the extent of reaction was monitored by TLC analysis (silica, CH_3CN/saturated aqueous KNO_3/water 7:1:0.5). Further heating for 18 h allowed the reaction to proceed to completion. The formation of a fine pink precipitate was observed. The mixture was cooled to room temperature, and water (2 cm^3) was added to dissolve the precipitate (as the bromide salt). The solution was reduced in volume to 5 cm^3, and a saturated methanolic solution of NH_4PF_6 was added to precipitate the product as the hexafluorophosphate salt. After filtration through Celite, the pink solid was washed with a small amount of cold CH_3OH, followed by water to remove excess NH_4PF_6. The Celite was washed with CH_3CN to remove the product, and solvent was removed. Complex **7**-$[PF_6]_4$ was isolated as a pink powder (29 mg, 72%). A small amount of solid K_2CO_3 was added to the NMR tube which was left standing for several hours. ES-MS: m/z: 1334 $[M-CH_2C_6H_4tpy-2PF_6]^+$, 867 $[Ru(pytpy)_2(PF_6)]^+$, 722 $[Ru(pytpy)_2]^+$, 632 $[pytpyCH_2C_6H_4tpy]^+$, 362 $[Ru(pytpy)_2]^{2+}$; ^{1}H NMR (500 MHz, CD_3CN): $\delta=9.18$ (s, 4H; H^{3B}), 9.17 (d, $J=6.5$ Hz, 4H; H^{2C}), 8.80 (d, $J=7.0$ Hz, 4H; H^{3C}), 8.79 (s, 4H; H^{3E}), 8.74 (m, 4H; H^{6F}), 8.72 (d, $J=8.0$ Hz, 4H; H^{3F}), 8.70 (d, $J=8.0$ Hz, 4H; H^{3A}), 8.12 (d, $J=8.5$ Hz, 4H; H^{2D}), 8.04 (dt, $J=7.8$, 1.8 Hz, 4H; H^{4F}), 8.00 (dt, $J=8.0$, 1.5 Hz, 4H; H^{4A}), 7.81 (d, $J=8.5$ Hz, 4H; H^{3D}), 7.52 (ddd, $J=7.5$, 5.0, 1.0 Hz, 4H; H^{5F}), 7.43 (d, $J=5.5$ Hz, 4H; H^{6A}), 7.22 (ddd, $J=8.0$, 5.5, 1.0 Hz, 4H; H^{5A}), 6.01 ppm (s, 4H; CH_2). ^{13}C NMR (125 MHz, CD_3CN): $\delta=158.2$ ($C^{2B,2E}$), 156.85 (C^{4E}), 156.8 ($C^{4B/4C}$), 156.0 (C^{2F}), 154.1 (C^{2A}), 153.5 (C^{6A}), 150.0 (C^{6F}), 146.5 (C^{2C}), 141.9 ($C^{4B/4C}$), 140.7 (C^{1D}), 139.5 (C^{4A}), 139.0 (C^{4F}), 134.9 (C^{4D}), 131.2 (C^{3D}), 129.3 (C^{2D}), 128.9 (C^{5A}), 127.7 (C^{3C}), 126.0 (C^{3A}), 125.6 (C^{5F}), 123.3 (C^{3B}), 122.4 (C^{3F}), 119.7 (C^{3E}), 64.9 ppm (CH_2); UV/Vis (CH_3CN): λ_{max} (ε) = 249 (104.1×10^3), 275 (134.6×10^3), 511 nm (35.6×10^3 $dm^3mol^{-1}cm^{-1}$); IR (solid): $\tilde{\nu}=3648$ (w), 3069 (w), 1637 (s), 1604 (w), 1583 (m), 1469 (m), 1422 (s), 1391 (m), 1358 (m), 1292 (w), 1165 (m), 1090 (w), 825 (vs), 785 (vs), 751 (s), 740 cm^{-1} (s); elemental analysis calcd (%) for $C_{84}H_{60}N_{14}RuP_4F_{24}\cdot9H_2O$: C 47.9, H 3.7, N 9.3; found: C 47.7, H 3.5, N 9.3; E° (vs. Fc/Fc^+): +1.01, −0.99 (quasi-reversible reduction), −1.72 V (irreversible reduction).

Complex 11$[PF_6]_6$: $[Fe(pytpy)_2][PF_6]_2$ (114 mg, 0.118 mmol) was heated to reflux in CH_3CN (15 cm^3). A solution of **9** (20 mg, 0.059 mmol) was added over 6 h and heating was continued for another 72 h. A saturated aqueous solution of NH_4PF_6 was added to the blue reaction mixture and the precipitate that formed was collected by filtration. Column chromatography (silica, CH_3CN/saturated aqueous KNO_3/water 7:1:0.5) was used to separate the dark blue product, which was eluted as the third fraction. The volume of solvent in the fraction was reduced to half under vacuum, and a solution of aqueous NH_4PF_6 was added to precipitate **11**$[PF_6]_6$, which was separated by filtration. This process was repeated several times to ensure complete ion exchange. Complex **11**$[PF_6]_6$ was isolated as a blue solid (33 mg, 23%). ES MS: m/z: 255 $[M-6PF_6]^{6+}$, 456 $[M-4PF_6]^{4+}$, 656 $[M-3PF_6]^{3+}$; ^{1}H NMR (250 MHz, CD_3CN): $\delta=9.32$ (s, 4H; H^{3F}), 9.26 (s, 4H; H^{3B}), 9.20 (d, $J=6.8$ Hz, 4H; H^{2C}), 9.03 (d, $J=$ 6.4 Hz, 4H; H^{3G}), 8.91 (d, $J=6.8$ Hz, 4H; H^{3C}), 8.65 (m, 8H; $H^{3E,3A}$), 8.24 (d, $J=5.9$ Hz, 4H; H^{2G}), 7.94 (m, 8H; $H^{4E,4A}$), 7.93 (d(AB), $J=8.3$ Hz, 4H; $H^{2D/3D}$), 7.77 (d(AB), $J=8.3$ Hz, 4H; $H^{3D/2D}$), 7.17 (m, 8H; $H^{6E,6A}$), 7.12 (m, 8H; $H^{5E,5A}$), 6.00 ppm (s, 4H; CH_2); E° (vs. Fc/Fc^+): +1.04, +0.79 V.

Complound 12$[PF_6]_2$: A mixture of pytpy (132 mg, 0.43 mmol) and **9** (70 mg, 0.21 mmol) in CH_3CN (10 cm^3) was heated at reflux for 4 h and then allowed to cool to room temperature. The white precipitate that formed was collected by filtration, was washed with CH_2Cl_2 and then was redissolved in CH_3OH. A saturated aqueous solution of NH_4PF_6 in CH_3OH (made slightly basic by addition of ten drops *N*-ethylmorpholine) was added, and the resulting precipitate was collected by filtration. After being washed with CH_2Cl_2, the product was dried under vacuum. Compound **12**$[PF_6]_2$ was isolated as a white solid (140 mg, 62%). M.p. 195–196°C; MALDI-TOF MS: m/z: 947 $[M-PF_6]^+$, 801 $[M-2PF_6]^+$; ^{1}H NMR (250 MHz, CD_3CN): $\delta=8.91$ (d, $J=6.8$ Hz, 4H; H^{6A}), 8.88 (s, 4H; H^{3B}), 8.73 (m, 8H; $H^{3C,2C/3A}$), 8.50 (d, $J=6.8$ Hz, 4H; $H^{2C/3A}$), 8.01 (ddd, $J=7.8$, 2.0 Hz, 4H; H^{4A}), 7.80 (d, $J=8.8$ Hz, 4H; $H^{2D/3D}$), 7.59 (d, $J=8.3$ Hz, 4H; $H^{2D/3D}$), 7.55 (m, 4H; H^{5A}), 5.83 ppm (s, 4H; CH_2); UV/Vis (CH_3CN): λ_{max} (ε) = 336 (7.6×10^3), 272 nm (73.1×10^3 $dm^3mol^{-1}cm^{-1}$); IR (KBr): $\tilde{\nu}=3125$ (w), 3103 (w), 3058 (w), 1639 (m), 1606 (w), 1585 (m), 1567 (w), 1549 (w), 1519 (w), 1471 (w), 1395 (m), 1155 (w), 840 (s; PF_6^-), 791 (m), 781 (m), 740 (w), 558 cm^{-1} (m; PF_6^-); elemental analysis calcd (%) for $C_{54}H_{40}F_{12}N_8P_2\cdot6H_2O$: C 54.10, H 4.37, N 9.35; found: C 54.31, H 4.32, N 9.24%.

Compound 13[PF_6]$_2$: A mixture of pytpy (116 mg, 0.37 mmol) and **10** (60 mg, 0.17 mmol) in CH_3CN (10 cm^3) was heated under reflux for 6 h. Workup and purification was as for **12**[PF_6]$_2$; compound [**13**][PF_6]$_2$ was isolated as a white solid (103 mg, 55%). MALDI-TOF MS: m/z: 959 $[M-PF_6]^+$, 502 $[M-\text{pytpy}-2PF_6]^+$; ^{1}H NMR (250 MHz, CD_3CN): $\delta=$ 8.84 (d, $J=7.0$ Hz, 4H; H^{2C}), 8.79 (s, 4H; H^{3B}), 8.67 (m, 4H; H^{6A}), 8.66 (m, 4H; H^{3A}), 8.42 (d, $J=7.0$ Hz, 4H; H^{3C}), 7.96 (dt, $J=7.8$, 1.5 Hz, 4H; H^{4A}), 7.44 (m, 4H; H^{5A}), 7.40 (d(AB), $J=8.5$ Hz, 4H; $H^{2D/3D}$), 7.36 (d(AB), $J=8.5$ Hz, 4H; $H^{3D/2D}$), 5.72 (s, 4H; NCH_2), 4.04 ppm (s, 2H; CH_2); IR (KBr): $\tilde{\nu}=$3126 (w), 3103 (w), 3060 (w), 3028 (w), 1639 (m), 1606 (w), 1585 (m), 1568 (w), 1549 (m), 1516 (w), 1471 (w), 1395 (m), 1155 (w), 841 (s; PF_6^-), 791 (m), 781 (m), 740 (w), 558 cm^{-1} (m; PF_6^-).

Complex 14[PF_6]$_8$: Nitrogen-purged solutions of **13**[PF_6]$_2$ (75 mg, 0.069 mmol) in CH_3CN (500 cm^3) and $Fe(BF_4)_2\cdot 6H_2O$ (23 mg, 0.068 mmol) in CH_3OH (500 cm^3) were added simultaneously to a stirred mixture of CH_3OH and CH_3CN (1:1, 500 cm^3) over a four day period at room temperature. The volume of solvent was then reduced to 500 cm^3 under vacuum, and a saturated aqueous solution of NH_4PF_6 was added. A blue precipitate formed and was collected by filtration. This was dissolved in CH_3CN and a saturated aqueous solution of KNO_3 was added; the precipitate formed was removed by filtration leaving an enriched solution of the desired product. The procedure was repeated until TLC (silica, CH_3CN/saturated aqueous KNO_3/H_2O 7:2:2) showed the presence of a single product ($R_f=0.32$). Aqueous NH_4PF_6 was added to a solution of the product in CH_3CN and the precipitate that formed was collected by fitration. This step was repeated several times to ensure that anion exchange was complete. The final precipitate was dissolved in a mixture of CH_3CN and CH_3OH (1:1, 50 cm^3) and Et_2O was added until a blue precipitate formed and a colourless supernatent liquid were obtained; this step was repeated several times. Complex **14**[PF_6]$_8$ was obtained as a blue solid (69 mg, 35%). ES-MS: m/z: 1291 $[M-2PF_6]^{2+}$, 813 $[M-3PF_6]^{3+}$, 573 $[M-4PF_6]^{4+}$, 430 $[M-5PF_6]^{5+}$, 334 $[M-6PF_6]^{6+}$; ^{1}H NMR (250 MHz, CD_3CN): $\delta=$9.16 (s, 8H; H^{3B}), 9.14 (d, $J=6.9$ Hz, 8H; H^{2C}), 8.76 (d, $J=6.6$ Hz, 8H; H^{3C}), 8.50 (d, $J=8.2$ Hz, 8H; H^{3A}), 7.83 (d, $J=8.5$ Hz, 8H; $H^{2D/3D}$), 7.80 (m, 8H; H^{4A}), 7.70 (d, $J=8.5$ Hz, 8H; $H^{3D/2D}$), 7.01 (m, 8H; H^{6A}), 6.99 (m, 8H; H^{5A}), 5.97 ppm (s, 8H; CH_2); UV/Vis (CH_3CN): λ_{max} (ε)=294 (157.8×10^3), 286 (150.8×10^3), 330 (54.1×10^3), 384 (17.7×10^3), 599 nm (46.8×10^3 $dm^3mol^{-1}cm^{-1}$); IR (KBr): $\tilde{\nu}=$1638 (s), 1608 (w), 1523 (w), 1425 (m), 1158 (w), 1091 (w), 838 (s; PF_6^-), 788 (m), 755 (w), 593 (w), 558 cm^{-1} (m; PF_6^-); E° (vs. Fc/Fc^+): +0.85, −1.09, −1.47, −1.76 V.

Complex 15[PF_6]$_8$: The method of preparation was as for complex **14**-[PF_6]$_8$ starting with [**13**][PF_6]$_2$ (30 mg, 0.027 mmol) and $Fe(BF_4)_2\cdot 6H_2O$ (10 mg, 0.030 mmol). Complex **15**[PF_6]$_8$ was collected as a blue powder (13 mg, 16%). ES-MS: m/z: 959 **13**+$PF_6]^+$, 822 $[M-3PF_6]^{3+}$, 580 $[M-4PF_6]^{4+}$, 407 $[\mathbf{13}]^{2+}$, 338 $[Fe(pytpy)_2]^{2+}$; ^{1}H NMR (600 MHz, CD_3CN): $\delta=$9.19 (s, 8H; H^{3B}), 9.03 (d, $J=6.5$ Hz, 8H; H^{2C}), 8.78 (d, $J=$ 7.0 Hz, 8H; H^{3C}), 8.44 (d, $J=8.0$ Hz,, 8H; H^{3A}), 7.57 (m, 16H; $H^{2D,3D}$), 7.44 (dt, $J=7.5$, 1.0 Hz, 8H; H^{4A}), 6.99 (d, $J=5.0$ Hz, 8H; H^{6A}), 6.52 (dt, $J=6.5$, 1.0 Hz, 8H; H^{5A}), 5.90 (s, 8H; NCH_2), 4.18 ppm (s, 4H; CH_2); UV/Vis (CH_3CN): λ_{max} (ε)=278 (132.4×10^3), 286 (131.8×10^3), 332 ($51.3\times$ 10^3), 379 (17.5×10^3), 595 nm (44.1×10^3 $dm^3mol^{-1}cm^{-1}$); IR (KBr): $\tilde{\nu}=$ 1639 (s), 1424 (m), 841 (s; PF_6^-), 790 (m), 559 cm^{-1} (m; PF_6^-). E° (vs. Fc/Fc^+): +0.86, −1.07, −1.33, −1.77 V.

Complex 16[PF_6]$_8$: Complex **2**[PF_6]$_2$ (23.2 mg, 0.023 mmol) and **10** (8.1 mg, 0.023 mmol) were dissolved in CH_3CN (20 cm^3) and the red solution was heated under reflux. After several hours, TLC analysis (silica, CH_3CN/saturated aqueous KNO_3/water 7:1:0.5) showed the presence of two pink spots with higher R_F values than the starting material. After 24 h, a further pink product (low $R_F=0.1$) was detected. Over the next 72 h, the amount of this material increased at the expense of both **2**[PF_6]$_2$ and the higher R_F pink fractions, until it became the dominant product. The solution was cooled to ambient temperature and the solvent was evaporated. Column chromatography (silica gel, CH_3CN/saturated aqueous KNO_3/water 7:1:0.5) was used to separate the components. The major product eluted very slowly, and elution was continued only until the product had separated fully from the head of the column. The product-containing silica was removed and suspended in CH_3CN/water (1:1, 30 cm^3). Solid NH_4PF_6 ($\approx$200 mg) was added, and the suspension was stirred until all of the silica was decolorised (30 min). The silica was removed by filtration, and the CH_3CN removed in vacuo leaving a pink precipitate. After filtering the suspension through Celite, the product was washed with water (50 cm^3) and then dissolved in CH_3CN. Solvent evaporation yielded **16**[PF_6]$_8$ as a dark pink solid (10 mg, 29%). MALDI TOF: m/z: 2701 $[M-2PF_6]^+$, 1482 $[(\text{tpy})Ru(\text{pytpy}CH_2C_6H_4CH_2C_6H_4CH_2\text{pytpy})Ru(\text{tpy})]^+$, 722 $[Ru(\text{pytpy})_2]^+$; ^{1}H NMR (500 MHz, CD_3CN): $\delta=$9.12 (s, 8H; H^{3B}), 9.00 (d, $J=7.0$ Hz, 8H; H^{2C}), 8.75 (d, $J=7.0$ Hz, 8H; H^{3C}), 8.55 (td, $J=8.0$, 1.5 Hz, 8H; H^{3A}), 7.55 (s, 16H; H^D), 7.54 (dt, $J=8.0$, 1.5 Hz, 8H; H^{4A}), 7.28 (ddd, $J=5.5$, 1.5, 0.5 Hz, 8H; H^{6A}), 6.63 (ddd, $J=7.5$, 5.5, 1.5 Hz, 8H; H^{5A}), 5.85 (s, 8H; NCH_2), 4.13 ppm (s, 4H; CH_2); ^{13}C NMR (125 MHz, CD_3CN): $\delta=$158.2 (C^{2A}), 156.5 (C^{2B}), 154.1 ($C^{4B/4C}$), 153.3 (C^{6A}), 146.1 (C^{2C}), 144.3 (C^{1D}), 142.1 ($C^{4C/4B}$), 138.9 (C^{4A}), 131.4 (C^{4D}), 130.9 ($C^{2D/3D}$), 130.7 ($C^{3D/2D}$), 128.4 (C^{5A}), 127.5 (C^{5C}), 125.9 (C^{3A}), 123.5 (C^{3B}), 64.9 (C_{NCH_2}), 41.9 ppm (C_{CH_2}); UV/Vis (CH_3CN): λ_{max} (ε)=222 (107.4×10^3), 236 (95.0×10^3), 274 (127.9×10^3), 311 (62.5×10^3), 340 (62.5×10^3), 507 nm (57.2×10^3 cm^{-1}); IR (solid): $\tilde{\nu}=$2966 (m), 2879 (m), 1473 (s), 1399 (m), 1045 (w), 880 (m), 832 (vs), 793 (m), 740 cm^{-1} (m); elemental analysis calcd (%) for $C_{110}H_{84}F_{48}N_{16}P_8Ru_2\cdot 5H_2O$: C 42.87, H 3.07, N 7.27; found C 42.87, H 3.26, N 7.14; E° (vs. Fc/Fc^+): +1.06, −1.03 (reversible reduction), −1.48(quasi-reversible reduction), −1.65 V (irreversible reduction).

X-ray crystal structure analysis of [3][PF_6]$_4\cdot$2(CH_3)$_2$CO·0.3CH_3CN: Determination of the cell parameters and collection of the reflection intensities were performed on an Enraf-Nonius Kappa CCD diffractometer (graphite monochromated $Mo_{K\alpha}$ radiation, $\lambda=0.71073$ Å). Purple plate, $0.12\times0.16\times0.47$ mm, monoclinic, space group $P2_1/n$, $a=8.9023(13)$, $b=$ 56.033(6), $c=14.1966(16)$ Å, $\beta=107.400(9)^\circ$, $T=173$ K, $V=$ 6757.5(15) Å^3, $Z=4$, $\rho_{calcd}=1.585$ g cm^{-3}, $\mu=0.442$ mm^{-1}, $F(000)=3250.4$. Number of reflections measured 55219 (unique 31808); 10733 observed reflections, $I>3\sigma(I)$, were used for the determination (1009 parameters); direct methods, Denzo/Scalepack,[60] SIR92.[61] CRYSTALS[62] was used for structure refinement. The refinement converged at $R=0.2294$ (all data), 0.0854 [observed $I>3\sigma(I)$], $wR=0.2301$ (all data), 0.0965 [observed $I>3\sigma(I)$], min and max residual electron density 1.88 and −1.45 e Å^{-3}; gof=1.123. CCDC-294985 contains the supplementary crystallographic data for this paper. These data can be obtained free of charge from The Cambridge Crystallographic Data Centre via www.ccdc.cam.ac.uk/data_request/cif.

Molecular modelling: Molecular mechanics calculations was carried out at the MM+ level using HyperChem release 7.0 (Hypercube Inc., 2002) in order to gain approximate structures of the iron(II) macrocyclic complexes.

Acknowledgements

We thank the Swiss National Science Foundation and the University of Basel for financial support. Sebastien Reymann is thanked for recording some of the ES mass spectra, and Jon Beves for recording some of the NMR spectra.

[1] R. P. Thummel, *Compr. Coord. Chem. II* **2004**, *1*, 41–53.
[2] E. C. Constable, *Adv. Inorg. Chem. Radiochem.* **1986**, *30*, 69–121.
[3] C. Kaes, A. Katz, M. W. Hosseini, *Chem. Rev.* **2000**, *100*, 3553–3590.
[4] E. C. Constable, *Education in Advanced Chemistry, Vol. 7, Perspectives in Coordination Chemistry* (Eds.: A. M. Trzeciak, P. Sobota, J. J. Ziolkowski) Poznan-Wroclaw University Publishing House (Wydawnictwa Uniwersytetu Wroclawskiego), **2000**, pp. 159–184.
[5] E. C. Constable, E. Schofield, *Chem. Commun.* **1998**, 403–404.
[6] G. U. Priimov, P. Moore, P. K. Maritim, P. K. Butalanyi, N. W. Alcock, *J. Chem. Soc. Dalton Trans.* **2000**, 445–449.
[7] G. R. Newkome, T. J. Cho, C. N. Moorefield, G. R. Baker, R. Cush, P. S. Russo, *Angew. Chem.* **1999**, *111*, 3899–3903; *Angew. Chem. Int. Ed.* **1999**, *38*, 3717–3721.

[8] G. R. Newkome, T. J. Cho, C. N. Moorefield, *Chem. Commun.* **2002**, 2164–2165.
[9] G. R. Newkome, T. J. Cho, C. N. Moorefield, R. Cush, P. S. Russo, L. A. Godínez, M. J. Saunders, P. Mohapatra, *Chem. Eur. J.* **2002**, *8*, 2946–2954.
[10] G. R. Newkome, T. J. Cho, C. N. Moorefield, P. P. Mohapatra, L. A. Godínez, *Chem. Eur. J.* **2004**, *10*, 1493–1500.
[11] P. Wang, C. N. Moorefield, G. R. Newkome, *Org. Lett.* **2004**, *6*, 1197–1200.
[12] G. R. Newkome, P. Wang, S.-H. Hwang, *Polym. Prepr.* **2005**, *46*, 1119–1120.
[13] S.-H. Hwang, C. N. Moorefield, F. R. Fronczek, O. Lukoyanova, L. Echegoyen, G. R. Newkome, *Chem. Commun.* **2005**, 713–715.
[14] P. Wang, C. N. Moorefield, G. R. Newkome, *Angew. Chem.* **2005**, *117*, 1707–1711; *Angew. Chem. Int. Ed.* **2005**, *44*, 1679–1683.
[15] C. B. Smith, E. C. Constable, C. E. Housecroft, B. M. Kariuki, *Chem. Commun.* **2002**, 2068–2069.
[16] E. C. Constable, C. E. Housecroft, C. B. Smith, *Inorg. Chem. Commun.* **2003**, *6*, 1011–1013.
[17] H. S. Chow, E. C. Constable, C. E. Housecroft, M. Neuburger, *Dalton Trans.* **2003**, 4568–4569.
[18] E. C. Constable, C. E. Housecroft, M. Neuburger, S. Schaffner, E. J. Shardlow, *Dalton Trans.* **2005**, 234–235.
[19] E. C. Constable, C. E. Housecroft, M. Neuburger, S. Schaffner, C. B. Smith, *Dalton Trans.* **2005**, 2259–2267.
[20] E. C. Constable, B. A. Hermann, C. E. Housecroft, M. Neuburger, S. Schaffner, L. J. Scherer, *New J. Chem.* **2005**, *29*, 1475–1481.
[21] H. S. Chow, E. C. Constable, C. E. Housecroft, M. Neuburger, S. Schaffner, *Polyhedron* **2006**, in press.
[22] H. Hofmeier, U. S. Schubert, *Chem. Soc. Rev.* **2004**, *33*, 373–399.
[23] H. Hofmeier, S. Schmatloch, U. S. Schubert, *Macromol. Chem. Phys.* **2003**, *204*, 2197–2203.
[24] S. Schmatloch, M. Fernández González, U. S. Schubert, *Macromol. Rapid Commun.* **2002**, *23*, 957–961.
[25] P. R. Andres, U. S. Schubert, *Adv. Mater.* **2004**, *16*, 1043–1068.
[26] U. S. Schubert, O. Hien, C. Eschbaumer, *Macromol. Rapid Commun.* **2000**, *21*, 1156–1161.
[27] P. R. Andres, U. S. Schubert, *Synthesis* **2004**, 1229–1238.
[28] P. R. Andres, U. S. Schubert, *Macromol. Rapid Commun.* **2004**, *25*, 1371–1375.
[29] E. C. Constable, A. M. W. Cargill Thompson, *J. Chem. Soc. Dalton Trans.* **1992**, 2947–2950.
[30] E. C. Constable, A. M. W. Cargill Thompson, *J. Chem. Soc. Dalton Trans.* **1994**, 1409–1418.
[31] E. Figgemeier, L. Merz, B. A. Hermann, Y. C. Zimmermann, C. E. Housecroft, H.-J. Güntherodt, E. C. Constable, *J. Phys. Chem. B* **2003**, *107*, 1157–1162.
[32] J. Paul, S. Spey, H. Adams, J. A. Thomas, *Inorg. Chim. Acta* **2004**, *357*, 2827–2832.
[33] J. P. López, W. Kraus, G. Reck, A. Thünemann, D. G. Kurth, *Inorg. Chem. Commun.* **2005**, *8*, 281–284.
[34] J. Granifo, M. T. Garland, R. Baggio, *Inorg. Chem. Commun.* **2004**, *7*, 77–81.
[35] L. Hou, D. Li, S. W. Ng, *Acta Crystallogr. Sect. E* **2004**, *60*, m1734–m1735.
[36] C. Metcalfe, S. Spey, H. Adams, J. A. Thomas, *J. Chem. Soc. Dalton Trans.* **2002**, 4732–4739.
[37] E. C. Constable, C. E. Housecroft, T. Kulke, C. Lazzarini, E. R. Schofield, Y. Zimmermann, *J. Chem. Soc. Dalton Trans.* **2001**, 2864–2871.
[38] S.-S. Sun, A. S. Silva, I. M. Brinn, A. J. Lees, *Inorg. Chem.* **2000**, *39*, 1344–1345.
[39] S.-S. Sun, A. J. Lees, *Inorg. Chem.* **2001**, *40*, 3154–3160.
[40] S. Hayami, K. Hashiguchi, G. Juhász, M. Ohba, H. Okawa, Y. Maeda, K. Kato, K. Osaka, M. Takata, K. Inoue, *Inorg. Chem.* **2004**, *43*, 4124–4126.
[41] L. Hou, D. Li, W.-J- Shi, Y.-G. Yin, S. W. Ng, *Inorg. Chem.* **2005**, *44*, 7825–7832.
[42] E. Figgemeier, E. C. Constable, C. E. Housecroft, Y. C. Zimmermann, *Langmuir* **2004**, *20*, 9242–9248.
[43] B. A. Hermann, L. J. Scherer, C. E. Housecroft, E. C. Constable, *Adv. Funct. Mater.* **2006**, *16*, 221–235.
[44] E. C. Constable, C. E. Housecroft, M. Neuburger, D. Phillips, P. R. Raithby, E. Schofield, E. Sparr, D. A. Tocher, M. Zehnder, Y. Zimmermann, *J. Chem. Soc. Dalton Trans.* **2000**, 2219–2228.
[45] W. Goodall, J. A. G. Williams, *J. Chem. Soc. Dalton Trans.* **2000**, 2893–2895.
[46] G. J. E. Davidson, S. J. Loeb, *Dalton Trans.* **2003**, 4319–4323.
[47] D. G. Kurth, J. P. López, W.-F. Dong, *Chem. Commun.* **2005**, 2119–2121.
[48] S. Liu, D. Volkmer, D. G. Kurth, *Pure Appl. Chem.* **2004**, *76*, 1847–1867.
[49] D. G. Kurth, D. Volkmer, R. V. Klitzing, *Multilayer Thin Films* **2003**, 393–426.
[50] D. G. Kurth, *Ann. N. Y. Acad. of Sci.* **2002**, *960* , 29–38 (Molecular Electronics II).
[51] D. Philp, J. F. Stoddart, *Angew. Chem.* **1996**, *108*, 1242–1286; *Angew. Chem. Int. Ed. Engl.* **1996**, *35*, 1154–1196.
[52] W. B. Jennings, B. M. Farrell, J. F. Malone, *Acc. Chem. Res.* **2001**, *34*, 885–894.
[53] M. Nishio, *CrystEngComm* **2004**, *6*, 130–158.
[54] M. J. Plater, T. Jackson, *Tetrahedron* **2003**, *59*, 4673–4685.
[55] H. Steinberg, D. J. Cram, *J. Am. Chem. Soc.* **1952**, *74*, 5388–5391.
[56] A. J. Blacker, J. Jazwinski, J.-M- Lehn, *Helv. Chim. Acta* **1987**, *70*, 1–12.
[57] W. Spahni, G. Calzaferri, *Helv. Chim. Acta* **1984**, *67*, 450–454.
[58] M. L. Turonek, P. Moore, W. Errington, *J. Chem. Soc. Dalton Trans.* **2000**, 441–444.
[59] J.-P- Collin, S. Guillerez, J.-P- Sauvage, F. Barigelletti, L. De Cola, L. Flamigni, V. Balzani, *Inorg. Chem.* **1991**, *30*, 4230–4238.
[60] Z. Otwinowski, W. Minor, *Methods Enzymol.* **1997**, *276*, 307–326.
[61] A. Altomare, G. Cascarano, G. Giacovazzo, A. Guagliardi, M. C. Burla, G. Polidori, M. Camalli, *J. Appl. Crystallogr.* **1994**, *27*, 435–435.
[62] P. W. Betteridge, J. R. Carruthers, R. I. Cooper, K. Prout, D. J. Watkin, *J. Appl. Crystallogr.* **2003**, *36*, 1487–1487.

Received: January 17, 2006
Published online: March 24, 2006

